

STUDY ON THE SENSITIVITY OF FUNCTIONALIZED NANOWIRES USING VARIED CHEMICALS

Chun-Chun Hsu Shu-Ping Lin*

ABSTRACT

Silicon nanowire-based metal-oxide-semiconductor field-effect transistors (SiNW MOSFETs) have been demonstrated excellent sensitivity and stability after surface modification and functionalization of nanowires. Chemical molecules have been applied to functionalize the surface of silicon surface. Silane coupling agents are good candidates for forming self-assembled monolayers (SAMs) by chemically interacting with silicon oxide. Those chemically modified SAMs can provide a functional surface to further conjugate biomolecules on SiNW MOSFETs. After functionalization, SiNW MOSFETs with tunably biocompatible surface can sustain a functional biointerface for biological tests. In this work, SiNW MOSFETs were fabricated using the standard I-line stepper of MOS semiconducting process and then visualized by scanning electron microscopy (SEM). The n-type SiNW MOSFETs devices were fabricated after the process of trimming, the scale of nanowire was down to a level of approximate 165 nm. 3-aminopropyl trimethoxysilane (APTMS) and 3-mercaptopropyl trimethoxysilane (MPTMS) SAMs were independently used to modify the surface of SiNW MOSFETs for pH sensing in biological buffer solution. Atomic force microscopy (AFM) and electron spectroscopy for chemical analysis (ESCA) were applied to characterize before and after surface modification. AFM found APTMS and MPTMS were successfully modified on silicon substrates. The average vertical length of APTMS and MPTMS SAMs from our AFM observation was around 2.628 nm and 2.698 nm, respectively. ESCA showed the specifically functional amino (-NH₂) groups and mercapto (-SH) groups on each APTMS and MPTMS modified silicon substrates. The specific amine functional group at 399.4 eV occurred after the modification of APTMS on silicon substrate in N1s spectra. S2p spectra showed the specific binding at 163.6 eV (C-SH) and 165.8 eV (-C-S-S-C-) after the modification of MPTMS on silicon substrate. Those disulfide bonds further influenced the organization of MPTMS-SAM on the surface; therefore, the APTMS had better SAM performance on our silicon substrate. On the other hand, electrical measuring system was used for elucidating that the suitable surface modification would have great impact on the sensing response and sensitivity. Varied biological PBS solutions at different pH values showed that unmodified SiNW MOSFETs were sensitive to the H⁺ ion change. When the pH level of the solution increased, the drain current of the unmodified SiNW MOSFETs decreased accordingly. In comparison with unmodified nanowires in current measurement, the changes of current of APTMS or MPTMS modified nanowires were enhanced in sensing of different pH solutions. Our results also showed that amino and mercapto groups of APTMS and MPTMS can improve the protonation and deprotonation reactions in different pH solutions. Both APTMS and MPTMS modified SiNW MOSFETs in pH sensings possessed good electrical sensing response and sensitivity in contrast with unmodified one. Moreover, in consequence of lower mercaptal groups of MPTMS on NWs,

Graduate Institute of Biomedical Engineering, National Chung Hsing University, Taichung 402, Taiwan, R. O. C.; 國立中興大學生物醫學工程研究所

* Corresponding author, E-mail: splin@dragon.nchu.edu.tw

DOI: 10.6287/JENCHU.2013.2403.04



the relatively minor signal responses to varied pH solutions in MPTMS modified SiNW MOSFETs. The electrical measurement showed that the amino groups of APTMS significantly improve the sensitivity of SiNW MOSFET in different pH sensings. Our results showed that adequate modification could provide a functionable surface for SiNW MOSFETs. We inferred the APTMS modified SiNW MOSFETs could be a real-time sensor for different pH levels detection and further applied in monitoring biological environment in the future.

Key words: MOSFET, silicon nanowire, surface modification, sensitivity.

1. INTRODUCTION

Silicon nanowire-based metal-oxide-semiconductor field-effect transistors (SiNW MOSFETs) have been explored in many biomedical aspects because of their high selectivity, extreme sensitivity, rapid response, and potential for integration into full electronic on-chip systems for high-throughput biological analyses [1-3]. The sensing mechanism of MOSFETs is the external localized field, such as charged molecules, influences carrier distribution in the near surface region of a sensing area. Because of the high surface to volume ratio and tunable electron transport properties due to quantum confinement effect [2], the electrical signals of NWs are sensitive to respond externally minor perturbation.

Techniques of surface modification have been applied to functionalize the surface of silicon. Silane coupling agents, such as 3-aminopropyltrimethoxysilane (APTMS) and 3-mercaptopropyl trimethoxysilane (MPTMS), are good candidates for forming self-assembled monolayers (SAMs) by chemically interacting with silicon oxide. Those chemically modified SAMs can provide a functional surface to further conjugate biomolecules on SiNW MOSFETs [4-7]. After functionalization, SiNW MOSFETs with tunably biocompatible surface can sustain a functional biointerface for biological tests. In addition, this biointerface can contribute better electrical signal to specific detection [8-10]. Lieber's group has showed highly sensitive SiNWs sensors based on electrical measurements for real-time detection of biological and chemical molecules. In addition, the electrical conductance exhibited pH-dependent trend and good linearity over a wide dynamic range in amine-functionalized SiNWs [2, 8, 11].

In this work, SiNW MOSFETs were fabricated using the standard I-line stepper of MOS semiconducting process and then visualized by scanning electron microscopy (SEM). APTMS and MPTMS SAMs were

then respectively utilized to modify silicon oxide surface of nanowires. The amino ($-NH_2$) groups of APTMS and mercapto ($-SH$) groups of MPTMS contributed a functional interface for sensing varied pH solutions. Each modified SiNW surfaces were characterized by atomic force microscopy (AFM) and electron spectroscopy for chemical analysis (ESCA). The electrical test and pH level detection in varied biological buffer solutions using unmodified and modified SiNW MOSFETs were recorded by electrical measuring system.

2. EXPERIMENTAL PROCEDURES

2.1 Materials

6-inch polished prime silicon wafers (boron doped) were purchased from MEMC Electronic Materials, Inc. All chemicals and reagents used in this study were purchased from Sigma-Aldrich. Polydimethylsiloxane (PDMS) were purchased from Dow Corning Corporation. The instrument for electrical measurement was semiconductor parameter analyzer (HP 4145B). Phosphate buffered solution (PBS) used in biological researches was purchased from Biowest.

2.2 Fabrication of SiNW MOSFETs

SiNW MOSFETs devices were fabricated at the National Nano Device Laboratories (Hsinchu, Taiwan). The process of fabrication of n-type SiNW MOSFETs devices was shown in Figure 1. An additional 100-nm polysilicon layer was deposited using the CVD process. Subsequently, the poly-Si nanowires were created by the standard I-line stepper of the MOS semiconducting process. The photoresist trimming and polysilicon etching were respectively performed in a transformer coupled plasma (LAM TCP 9400 SE) with classical $HBr/Cl_2/O_2$ chemistry. A pattern of channel protection photoresist was then formed by I-line lithography to keep the nanowires from ion implantation of source/drain (S/D). The S/D

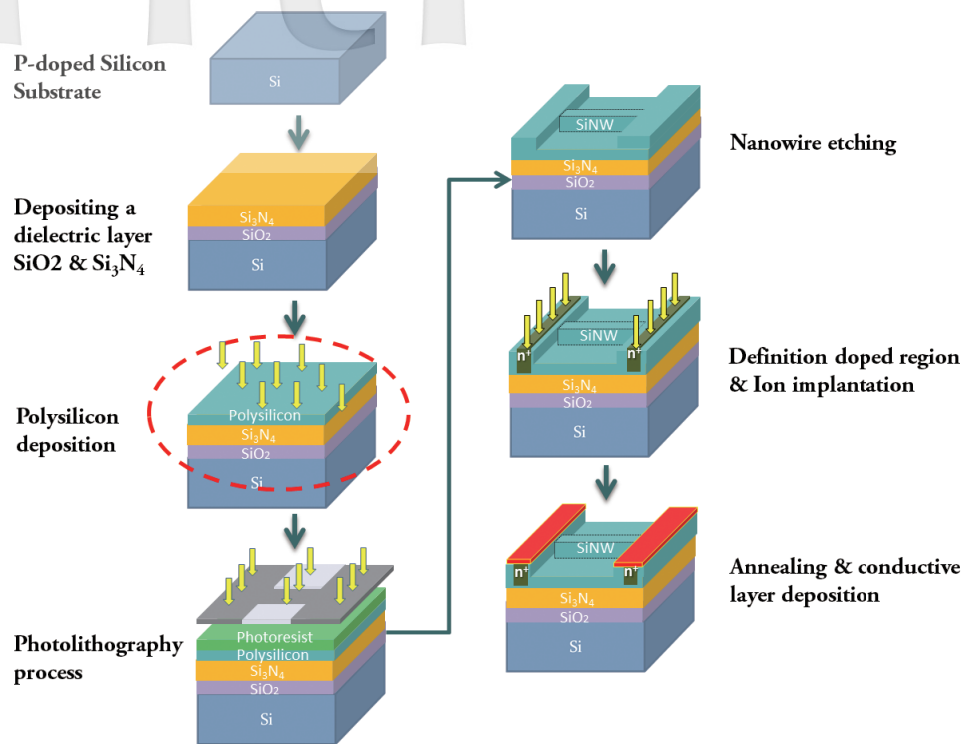


Figure 1. Fabrication process of SiNW MOSFETs.

pads were doped with a $1 \times 10^{22} \text{ cm}^{-3}$ phosphorus ion at 35 keV to reduce the parasitic resistance of the NW. Thereafter, the photoresist on channel protection was removed. The S/D dopants were activated by a rapid thermal anneal step at 900°C for 30 min in N₂ ambience. Metal contacts were created by deposition of Ni/Ti layers on S/D pads. The devices were then annealed at 400°C for 3 hr in N₂ ambience to construct a reliable metal/silicon ohmic contact. The SiNW MOSFETs were observed using SEM (JSM-6700F, JEOL). All the specimens of SiNW MOSFETs were deposited a thin layer of gold using a sputter coater (Auto 108, Cressington, Watford, UK) before SEM examination.

2.3 Fabrication of Microfluidic Channels

We utilized microfluidic channel made of PDMS to surface modify molecules on SiNWs surface and to further introduce all the analytes. PDMS microfluidic channel was then placed on the top of the device to flow the intended molecules of aqueous solutions through SiNWs. The mold of microfluidic channels was created by using conventional photolithography method in Figure 2. The SU-8 photoresist was first coated on the glass substrate. The main mold of microfluidic channels was then fabricated after the processes of exposure

and development. The liquid PDMS was subsequently poured into mold, and the specific pattern of microfluidic channels was created.

2.4 Functionalization and Characterization of SiNW MOSFETs

SiNWs were independently modified with small silanol chemicals, i.e. APTMS and MPTMS, to provide functional groups on the sensing areas. First, the chips and microfluidic channels were washed by pure ethanol and then heated at 120°C for 5 min to remove the surplus ethanol. After that, the nanowires were respectively modified with 1.0% ethanolic solution of APTMS and MPTMS for 1 hr. After the modification, the samples were rinsed with anhydrous ethanol for several times and then heated in ethanol in an oven at 60°C for 5 min. All the samples were blown dry with pure N₂ gas. The APTMS and MPTMS-SAMs modified SiNW MOSFETs were ready for pH sensing by using electrical measurement.

AFM (Veeco Dimension 5000 Scanning Probe Microscope) was used to scan the surface morphology of the each-step modification of silicon surface. The AFM images were collected in tapping mode. The Si tips (Nanosensors, PointProbePlus-RT-NCHR, tip curvature radius < 7 nm) were utilized to scan the 2D/3D

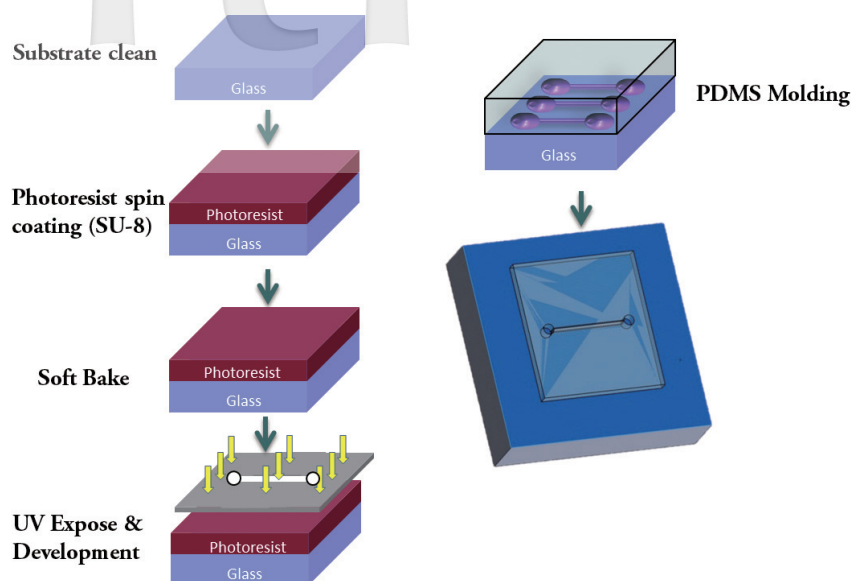


Figure 2. Fabrication process of microfluidic channels.

morphology and roughness of the surface.

ESCA was utilized to analyze the elemental composition and characterize specific chemical bonding in each-step modification of SiNW MOSFET. The ESCA spectra were acquired with a VG Scientific Microlab 310F, a micro-focus non-monochromatic aluminum anode (Al [K α] 1,486.6 eV), and a Concentric Hemispherical Analyzer. Chemical survey scanning was depicted, and it then showed the chemical elements of each samples. The C1s, N1s and S2p core level spectra were measured and fitted by using Voigt peak profiles and a Shirley background together with a database for semiconductor and organic polymer.

2.5 Electrical Measurement of SiNW MOSFETs

The characteristics of SiNW MOSFETs and pH sensing were measured by source-monitor-unit system (HP 4145B), the back gate potential and source-drain bias voltage were controlled. Generally, the drain current (I_d) was measured at several constant bias voltages, V_g from -3.0 to 3.0 V with a step of 1.0 V. The drain voltage (V_d) was swept from -5.0 to 5.0 V to test the performance of SiNW MOSFETs. Varied pH solutions of PBS commonly used in biological research were applied in pH sensing studies. The PBS solutions of pH 2, pH 4, pH 7, pH 9 and pH 11 were introduced to raw or modified SiNWs using microfluidic channel for examination the electrical response of unmodified and modified SiNW MOSFETs.

3. RESULTS AND DISCUSSION

3.1 Characterization of SiNW MOSFETs and Microfluidic

The n-type SiNW MOSFETs devices were fabricated based on standard I-line stepper of the MOS semiconducting process. In Figure 3 (a) showed the original width of NWs was ~ 304 nm. After the process of trimming, the scale of nanowire was down to a level of approximate 165 nm in Figure 3 (b). Figure 3 (c) and (d) showed the top-view appearance and AFM morphology of SiNW MOSFET device, respectively.

Figure 4 (a) showed the mask design of the microfluidic channel, Figure 4 (a), (b) and (c) showed the actual dimension of microfluidic channels ($16 \text{ mm} \times 0.5 \text{ mm} \times 0.35 \text{ mm}$) fabricated by PDMS. The microfluidic channel was used to introduce all the solutions in this study.

3.2 Surface Characterization of SiNW MOSFETs

Surface topographies of the SiNW MOSFETs before and after each-step modification were scanned by AFM. Prior to the surface modification, the AFM images showed the interface between modified and unmodified areas. After functionalization of APTMS and MPTMS on silicon surface, the modified areas of AFM images can be seen in Figure 5 (a) and (b), respectively. Our results showed both APTMS and MPTMS could form a SAM and further functionalize the silicon substrates. However, the MPTMS SAM was easier to form crystalline and stacked on the

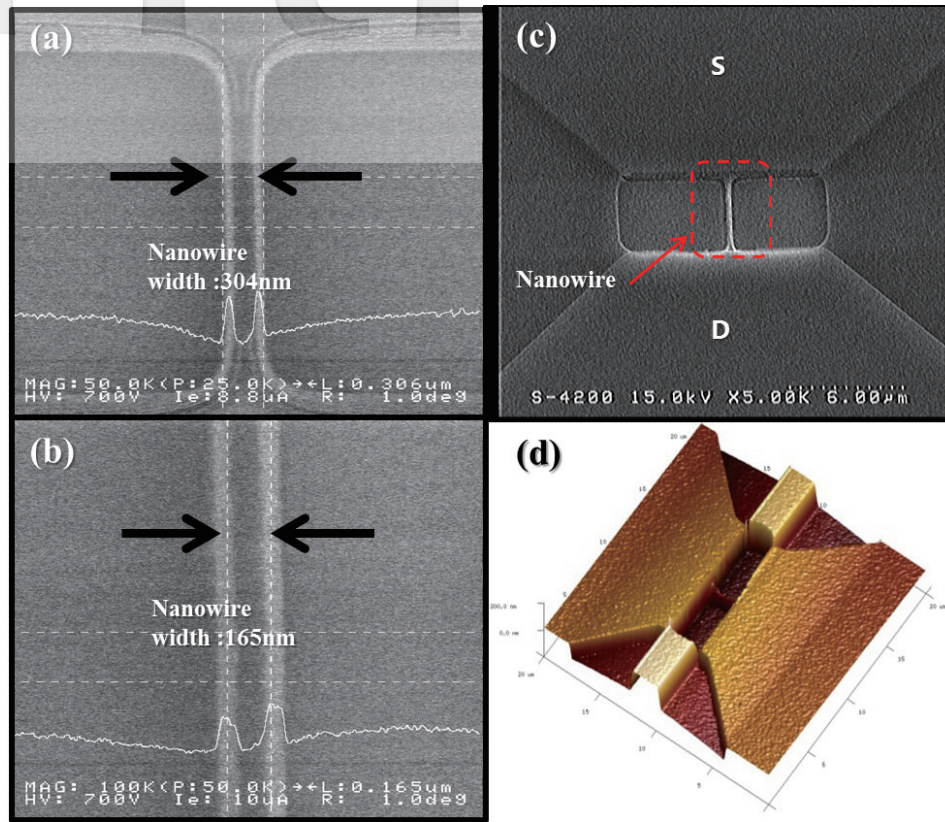


Figure 3. SEM and AFM images of SiNW MOSFET device. (a) SEM analysis for visualizing Si-nanowire width, the width of nanowire was 304 nm before trimming. (b) After trimming, the width of nanowire was 165 nm. (c) and (d) showed the top-view appearance and AFM morphology of SiNW MOSFET device, respectively.

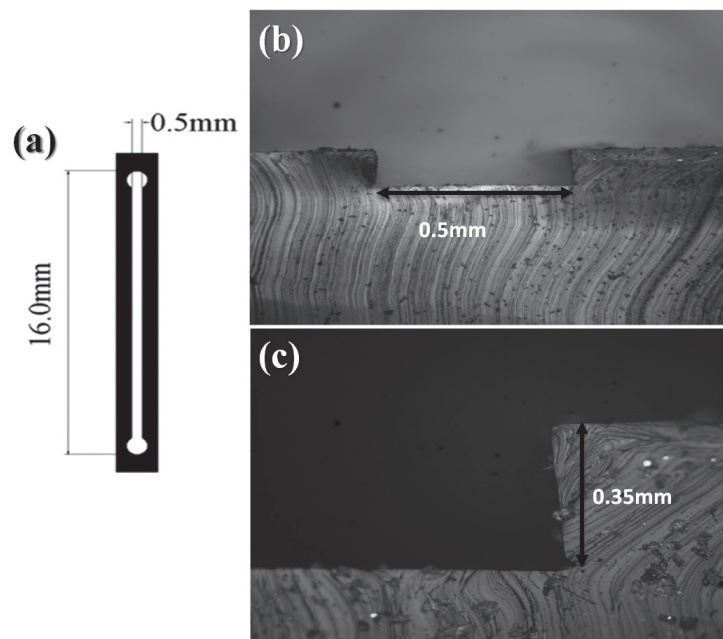


Figure 4. (a) Showed the mask design of microfluidic channel. Cross-sectional views of microfluidic channel were showed at the magnification of (b) 200x and (c) 500x under optical microscope.

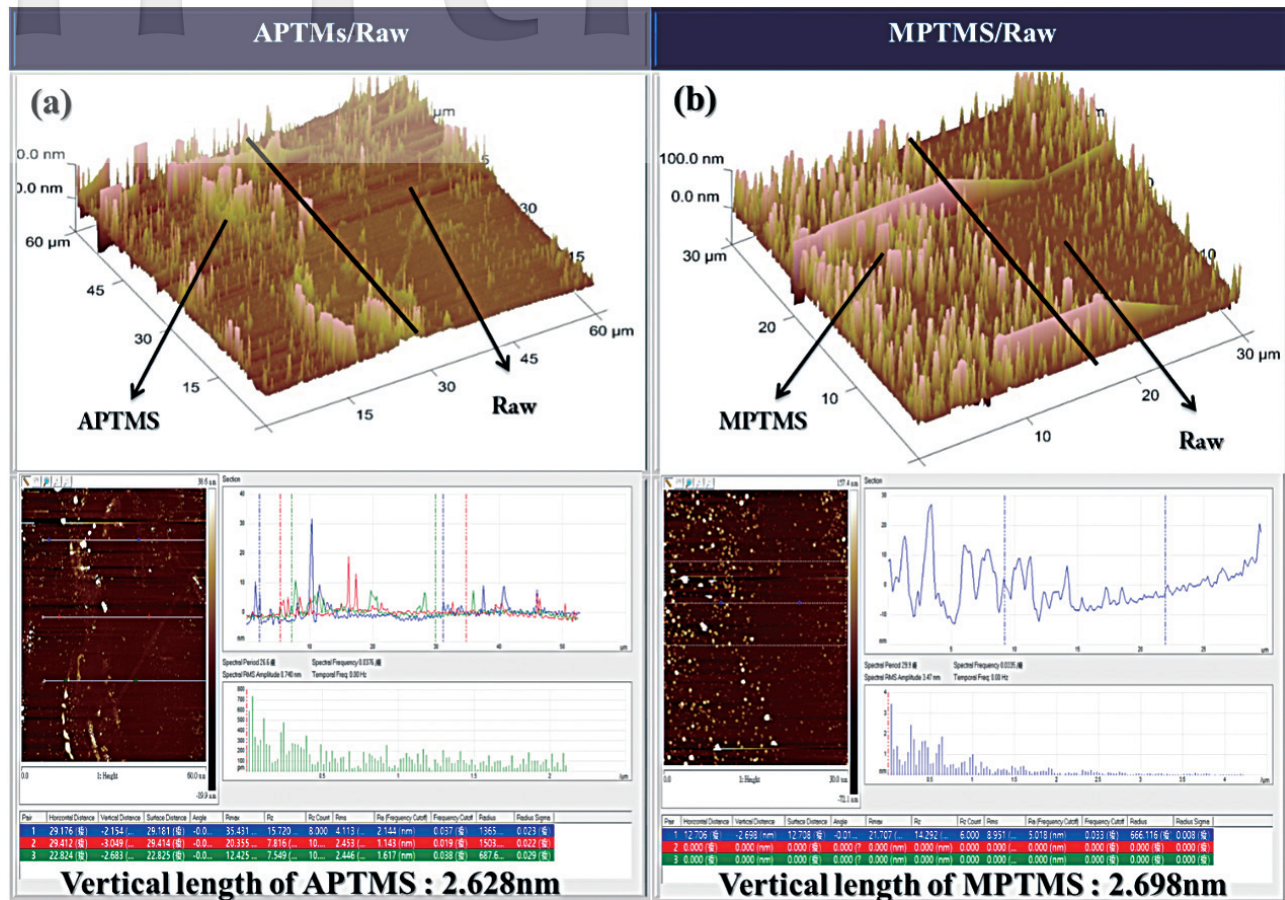


Figure 5. AFM images showed the interface between raw silicon and SAM modified area. (a) and (b) were the interface between APTMS and raw silicon substrate and the interface between MPTMS and raw silicon substrate, respectively.

silicon surface. The average vertical length of APTMS and MPTMS SAMs from our AFM observation was around 2.628 nm and 2.698 nm, respectively.

The chemical composition and the specific chemical structure in each-step modification of silicon surfaces were identified by the ESCA and shown in Figure 6. The specifically chemical elements were appeared on raw silicon (Figure 6 [a]), APTMS-modified (Figure 6 [b]) and MPTMS-modified (Figure 6 [c]) silicon substrates. After APTMS and MPTMS modified the silicon substrates, the specific carbon, nitrogen and sulfur elements appeared. Furthermore, Figure 6 (d) and (e) shows the N1s spectra before and after modification of APTMS, the specific amine functional group at 399.4 eV occurred after the modification of APTMS on silicon substrate. Figure 6 (f) and (g) shows the S2p spectra before and after modification of MPTMS. Figure 6 (g) showed the specific binding at 163.6 eV (C-SH) and

165.8 eV (-C-S-S-C-) after the modification of MPTMS on silicon substrate. Relatively bulky MPTMS SAM in AFM image (in Figure 5 [b]) might be attributed to the formation of disulfide bonding between the mercapto groups of MPTMS in ESCA examination [8]. Those disulfide bonds further influenced the organization of MPTMS-SAM on the surface; therefore, the APTMS had better SAM performance on our silicon substrate.

3.3 Electrical Characterization of Varied Functionalized SiNW MOSFETs

The SiNW MOSFETs device described above was verified by electrical characterization and shown in Figure 7. All electrical measurements were taken by SMU system. The I_d-V_d characteristics were obtained by sweeping the source drain voltage while the V_g was constant at 5 V. Figure 7 (a) and (b) showed a significantly different performance before and after annealing treatment. Output characteristics showed that the current between the source

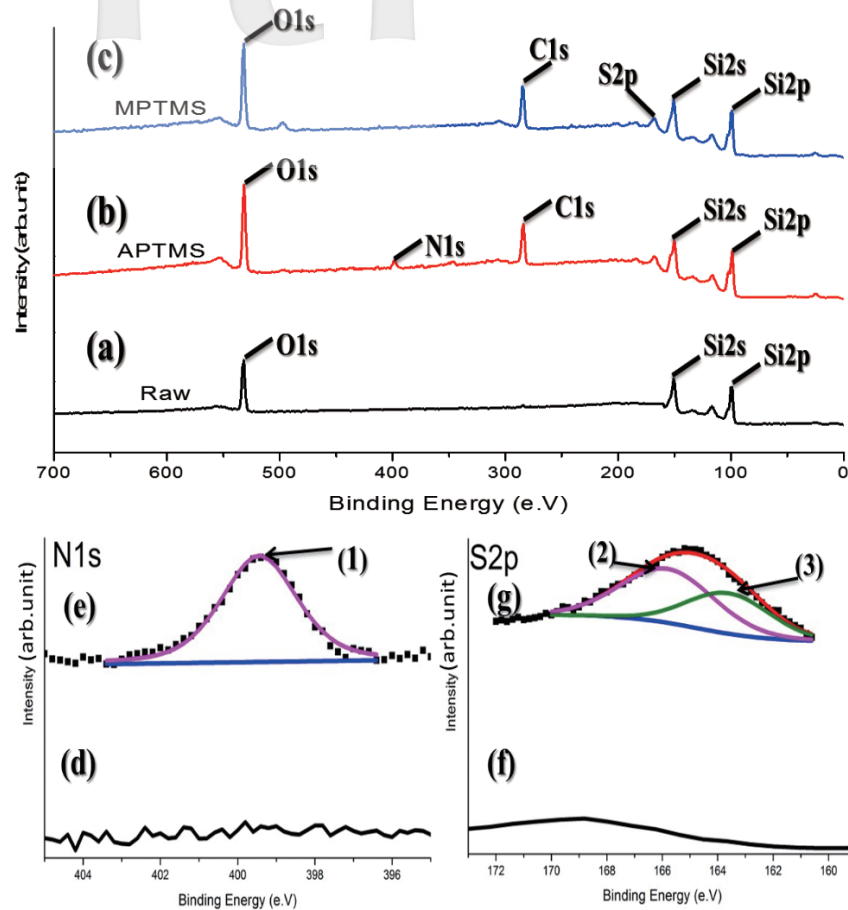


Figure 6. Survey scannings of before and after modifications were examined by ESCA and showed in (a) raw silicon wafer, (b) APTMS modification and (c) MPTMS modification, respectively. N1s and S2p XPS spectra were independently obtained from APTMS modified and MPTMS modified silicon nanowire. (d) and (e) showed N1s scanning of before and after APTMS modification of silicon substrates. (f) and (g) showed the S2p scanning of before and after MPTMS modification of APTMS. The deconvoluted peaks were fitted with the following binding energies: (1) 399.8 eV (C-NH_2), (2) 165.8 eV (-C-S-S-C-) and (3) 163.7 eV (C-SH).

and drain was controlled effectively by the gate electrodes as shown in Figure 7 (c).

Electrical measurement was used to verify that the varied functional groups pre- and postfunctionalization would have a great impact on the sensitivity of NW MOSFETs in our study. The results of pH sensing for biological PBS solutions at different pH values using unmodified, APTMS and MPTMS modified NW MOSFETs were shown in Figure 8. In Figure 8 (a), varied PBS solutions at different pH values showed that unmodified SiNW MOSFETs were sensitive to the H^+ ion change. When the pH level of the solution increased, the drain current of the unmodified SiNW MOSFETs decreased accordingly. In comparison with unmodified

nanowires, the changes of drain current of APTMS or MPTMS modified nanowires were enhanced in sensing of different pH solutions in Figure 8 (b). The results of pH sensing in Figure 8 (b) also showed that amino and mercapto groups of APTMS and MPTMS can improve the protonation and deprotonation reactions in different pH solutions. Figure 8 (c) shows the percentages of sensitivity changes of raw, APTMS modified, and MPTMS modified nanowire in drain-current measurement, it further displayed APTMS modified SiNW MOSFETs significant improved the sensitivity and had promising signal response. It has been demonstrated that MPTMS-SAM modified on SiNW MOSFETs might form disulfide bonding between the mercapto groups of MPTMS in our AFM scanning and

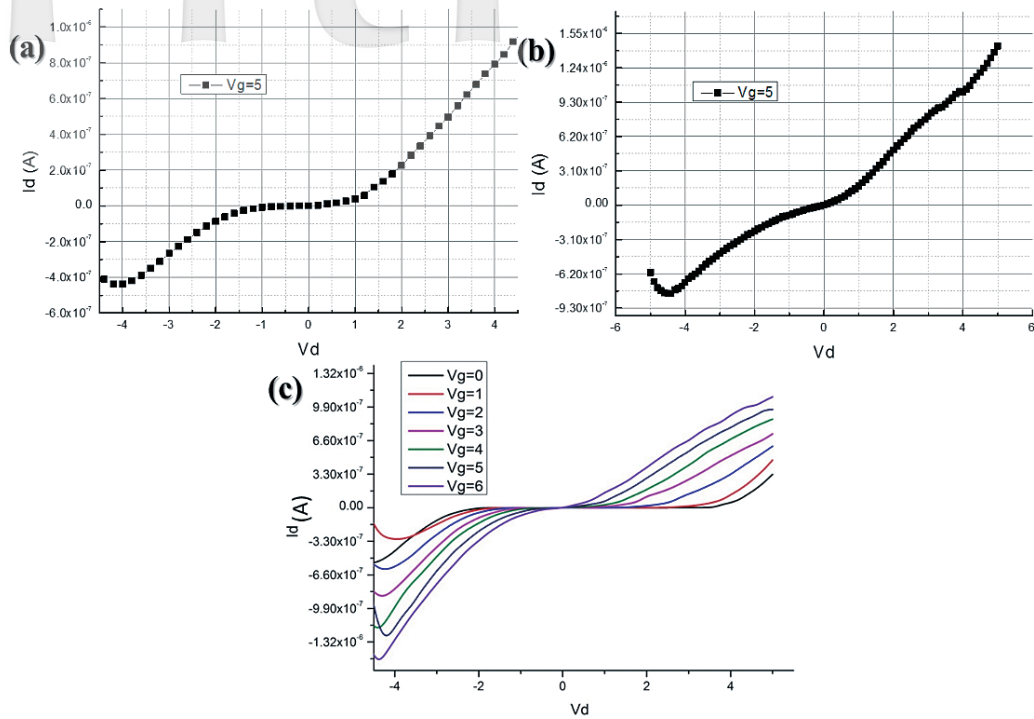


Figure 7. I_d - V_d curve of (a) before annealing treatment and (b) after 400°C N_2 annealing treatment showed the characteristics of SiNW MOSFETs. (c) I_d - V_d curve showed the current was controlled by the gate bias.

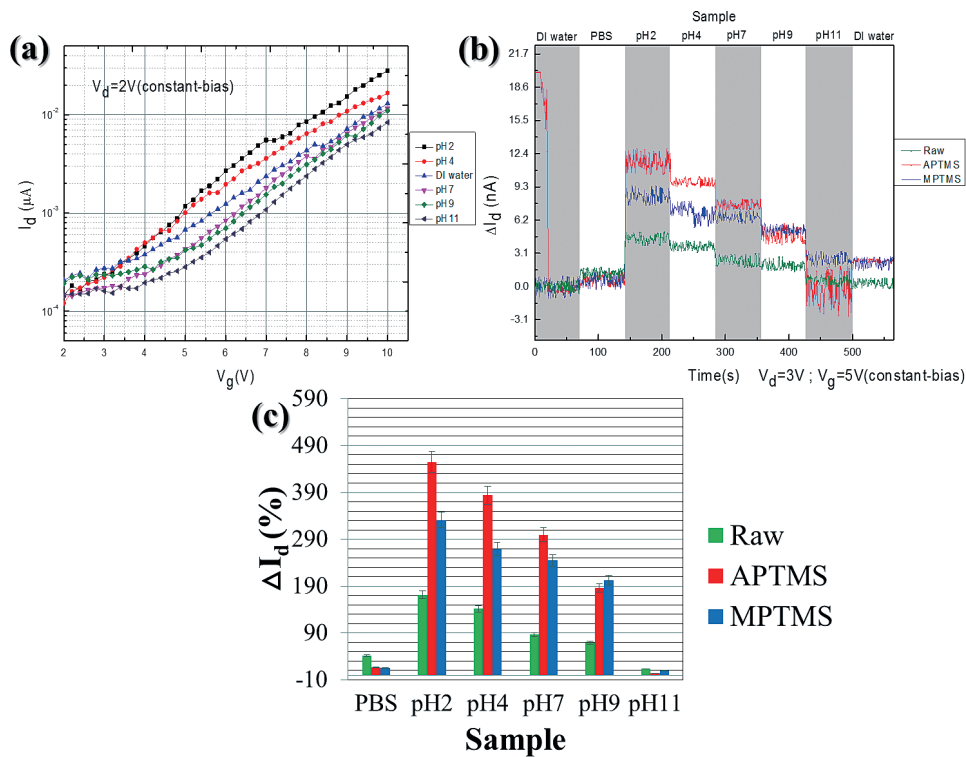


Figure 8. Electrical measurements for biological PBS solutions at different pH values. (a) The changes of I_d - V_d were recorded by using raw SiNW MOSFETs. (b) The changes of I_d at varied pH levels were recorded by using raw, APTMS and MPTMS modified SiNW MOSFETs. (c) The percentages of sensitivity changes of current were observed ($N = 6$).

ESCA examination. In consequence of lower mercaptal groups of MPTMS on NWs, the relatively minor signal responses to varied pH solutions were found in Figure 8 (c). In addition, the processes of our SiNW MOSFETs fabrication and surface modification can enhance the overall sensitivity of signal response to varied pH level in contrast with other studies [4, 12].

4. CONCLUSION

The results of AFM and ESCA showed that the modifications of APTMS and MPTMS SAMs could successfully functionalize the surface of SiNW. In addition, these functionable SAMs are sensitive to the external pH changes in our electrical measurement. Furthermore, the electrical measurement showed that the amino groups of APTMS improve the sensitivity of SiNW MOSFET in different pH sensings. We found that adequate modification could provide a functionable surface for SiNW MOSFETs. Our results inferred the APTMS modified SiNW MOSFETs could be a real-time sensor for different pH levels detection and further applied in monitoring biological environment in the future.

ACKNOWLEDGMENTS

The authors thank Prof. Chun-Ping Jen from National Chung Cheng University for useful discussions. Technical support to fabricate microfluidic channels and the silicon NW-MOSFETs were given by the Center of Nanoscience and Nanotechnology at National Chung Hsing University and National Nano Device Laboratories in Taiwan, respectively. This work was supported by the National Science Council of Taiwan under contract number NSC 100-2221-E-005-016-, NSC 101-2221-E-005-002- and NSC 101-2923-E-005-001-MY3.

REFERENCES

- Grieshaber, D., MacKenzie, R., Vörös, J. and Reimhult, E., "Electrochemical Biosensors -- Sensor Principles and Architectures," *Sensors*, Vol. 8, No. 3, pp. 1400-1458 (2008).
- Huang, X.-J. and Choi, Y.-K., "Chemical Sensors Based on Nanostructured Materials," *Sensors and Actuators B: Chemical*, Vol. 122, No. 2, pp. 659-671 (2007).
- Park, I., Li, Z., Pisano, A.P. and Williams, R.S., "Top-Down Fabricated Silicon Nanowire Sensors for Real-Time Chemical Detection," *Nanotechnology*, Vol. 21, No. 1, pp. 015501-015501 (2010).
- Cui, Y., Wei, Q., Park, H. and Lieber, C.M., "Nanowire Nanosensors for Highly Sensitive and Selective Detection of Biological A Chemical Species," *Science*, Vol. 293, No. 5533, pp. 1289-1292 (2001).
- Timko, B.P., Cohen-Karni, T., Qing, Q., Tian, B. and Lieber, C.M., "Design and Implementation of Functional Nanoelectronic Interfaces with Biomolecules, Cells, and Tissue Using Nanowire Device Arrays," *IEEE Trans Nanotechnol*, Vol. 9, No. 3, pp. 269-280 (2010).
- Zheng, G., Patolsky, F., Cui, Y., Wang, W.U. and Lieber, C.M., "Multiplexed Electrical Detection of Cancer Markers with Nanowire Sensor Arrays," *Nature Biotechnology*, Vol. 23, pp. 1294-1301 (2005).
- Allen, G.C., Sorbello, F., Altavilla, C., Castorina, A. and Ciliberto, E., "Macro-, Micro- and Nano-Investigations on 3-Aminopropyltrimethoxysilane Self-Assembly-Monolayers," *Thin Solid Films*, Vol. 483, No. 1-2, pp. 306-311 (2005).
- Lin, S.P., Chi, T.Y., Lai, T.Y. and Liu, M.C., "Investigation into the Effect of Varied Functional Biointerfaces on Silicon Nanowire MOSFETs," *Sensors (Basel)*, Vol. 12, No. 12, pp. 16867-16878 (2012).
- Lin, S.-P., Pan, C.-Y., Tseng, K.-C., Lin, M.-C., Chen, C.-D., Tsai, C.-C., Yu, S.-H., Sun, Y.-C., Lin, T.-W. and Chen, Y.-T., "A Reversible Surface Functionalized Nanowire Transistor to Study Protein-Protein Interactions," *Nano Today*, Vol. 4, No. 3, pp. 235-243 (2009).
- Healy, D.A., Hayes, C.J., Leonard, P., McKenna, L. and O'Kennedy, R., "Biosensor Developments: Application to Prostate-Specific Antigen Detection," *Trends Biotechnol*, Vol. 25, No. 3, pp. 125-131 (2007).
- Aswal, D.K., Lenfant, S., Guerin, D., Yakhmi, J.V. and Vuillaume, D., "A Tunnel

Current in Self-Assembled Monolayers of 3-Mercaptopropyltrimethoxysilane,” *Small*, Vol. 1, No. 7, pp. 725-729 (2005).

12. Stern, E., Vacic, A., Li, C., Ishikawa, F.N., Zhou, C., Reed, M.A. and Fahmy, T. M., “A Nanoelectronic Enzyme-Linked Immunosorbent Assay for Detection of Proteins in Physiological Solutions,” *Small*, Vol. 6, No. 2, pp. 232-238 (2010).

Manuscript Received: Aug. 05, 2013

Revision Received: Aug. 31, 2013

and Accepted: Sep. 02, 2013